Letter

Exact large deviations and emergent long-range correlations in sequential quantum East circuits

Jimin Li,[1,*] Bruno Bertini,[2] Juan P. Garrahan,[3,4] and Robert L. Jack[1,5]
[1]*Department of Applied Mathematics and Theoretical Physics, University of Cambridge, Wilberforce Road, Cambridge CB3 0WA, United Kingdom*
[2]*School of Physics and Astronomy, University of Birmingham, Birmingham B15 2TT, United Kingdom*
[3]*School of Physics and Astronomy, University of Nottingham, Nottingham NG7 2RD, United Kingdom*
[4]*Centre for the Mathematics and Theoretical Physics of Quantum Non-Equilibrium Systems, University of Nottingham, Nottingham NG7 2RD, United Kingdom*
[5]*Yusuf Hamied Department of Chemistry, University of Cambridge, Lensfield Road, Cambridge CB2 1EW, United Kingdom*

(Received 24 September 2025; revised 22 December 2025; accepted 3 March 2026; published 27 March 2026)

Exploiting quantum measurements is a promising route for the preparation of correlated quantum states. We use methods from large deviation theory to solve this problem exactly for a specific system: the deterministic quantum East circuit with boundary measurements. We show that conditioning on measurement outcomes generates a long-range correlated state, despite typical trajectories being trivial. We derive the channel that optimally realizes the rare measurement trajectories, and establish a formal connection with the Petz recovery (time-reversal) map. We compute one- and two-point correlation functions in the conditioned state, revealing finite two-body correlations at arbitrarily large separations, and an underlying fractal structure, related to the Sierpiński triangle. These results demonstrate explicitly how boundary measurements can be used to control bulk properties of a quantum system.

DOI: 10.1103/72kx-56lt

Introduction. The current decade has witnessed the rise of quantum circuits—quantum many-body systems in discrete space and discrete time—as a new paradigm to understand out-of-equilibrium quantum matter [1–3]. In broad terms, this has occurred for three main reasons: (i) in circuit systems one can discard much unnecessary detail while maintaining only essential physical ingredients, such as the locality of interactions; (ii) the symmetry between space and time realized by quantum circuits offers more avenues for theoretical analysis of their dynamics [1–6]; and (iii) circuits do model accurately certain actual quantum devices [7–12].

A particularly significant research direction, facilitated by the discrete spacetime setting, has been studying the interplay of unitary dynamics and measurements. This raises both conceptual and practical questions for quantum dynamics and quantum computation: measurements can tame the growth of entanglement induced by unitary evolution, leading to much-studied phase transitions in conditioned states (see, e.g., Refs. [13–15]). Combining unitary dynamics and measurements can also allow for the preparation of states with nontrivial correlation patterns in circuits with low depths, which are practically implementable in current quantum devices (see, e.g., Refs. [16–22] and references therein). In this Letter, we present an example where the emergence of such an interesting quantum state can be shown exactly in the many-body setting.

We work in the framework of "collision models" [23–32] (a discrete time version of the input-output formalism [33–35]). Here, a quantum system is made to interact with a different ancilla at every step of the evolution, after which the ancilla is measured. As in other versions of quantum Markov chains, a collision model defines a quantum channel for the dynamics of the average state; it also yields an unraveling into quantum trajectories for the stochastic evolution of the state conditioned on the measurements [35–37]. Specifically, given the channel that defines the stochastic dynamics, the statistics of measurements and conditioned states are encoded by the tilted channel [38–40]. This works as follows: the outcomes of repeated measurements are summed over time, for each trajectory its probability is exponentially reweighted by these totals, and the reweighted probabilities added up. Hence one obtains the moment generating function of the counts, which coincides with the trace of the exponential of the tilted generator. Furthermore, the tilted ensemble of trajectories captures rare events of the dynamics via a form of postselection, leading to interesting properties in the conditioned state. In principle, this postselected ensemble can be sampled efficiently through a quantum Doob transformation [38,41], i.e., introducing the proper stochastic dynamics that generates the exponentially tilted probabilities. These methods are a generalization of large deviation theory [42] to quantum Markov chains [38,41,43].

Here, we consider a particular many-body collision model in which the analysis of the tilted channel can be carried out exactly and explicitly. The system consists of L system qubits and one ancilla qubit per time step. At each step the qubits

*Contact author: jl939@cam.ac.uk

Published by the American Physical Society under the terms of the Creative Commons Attribution 4.0 International license. Further distribution of this work must maintain attribution to the author(s) and the published article's title, journal citation, and DOI.

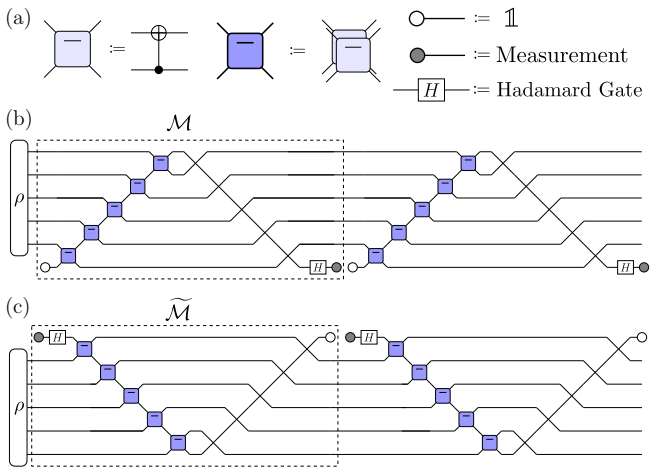


FIG. 1. Sequential quantum East circuits. (a) CNOT gate, its folded counterpart, and identity, (diagonal) measurement, and Hadamard matrices. (b) Sequential East circuit consisting of two iterations of the channel $\mathcal{M}$. The circuit acts on $L+1$ sites ($L=5$ in the figure), which couple an input on the first L sites to a maximally mixed ancilla. Measurements are performed at the ancilla. (c) Alternative circuit in which the ancilla is prepared in a nontrivial mixed state and traced after each application of the channel $\widetilde{\mathcal{M}}$.

are evolved by a sequential circuit of controlled-not (CNOT) (i.e., the gates of the quantum East circuit at its deterministic point [44–47]) and SWAP gates followed by a projective measurement of the ancilla in the Hadamard rotated basis (see Fig. 1). Note that in our setup the unitary evolution is implemented by an automaton circuit [3,48–54]. On average, the system is evolved by a unital channel, $\mathcal{M}$, whose trivial steady state lacks any correlations. However, as we prove exactly below, the behavior at the level of fluctuations is far from trivial: exponentially tilting according to measurement outcomes yields a conditional state of the system that is long-range correlated, and described by a linear-depth circuit. Furthermore, via the exact quantum Doob transform, we find a quantum circuit that reproduces these correlations in its typical trajectories and therefore in its steady state. Besides providing a controlled many-body setting for exact analysis of the interplay of measurements and unitary dynamics, our results also provide a realizable system that can be used to benchmark current quantum devices.

Setup. We consider a quantum channel $\mathcal{M}$ defined as the spacetime circuit shown in Figs. 1(a) and 1(b). Throughout we use the standard diagrammatic techniques of quantum circuits, and in particular we work in the folded representation (see, e.g., Ref. [3]), so that shapes with legs protruding from two (left and right) sides indicate superoperators and those with legs on one only (left or right) side are matrices (or operators). Figure 1 shows a circuit of $L=5$ qubits (the general L setup should be evident) but all our results are for arbitrary L.

The circuit of Figs. 1(a) and 1(b) describes the following dynamics: (i) prepare an ancilla in the maximally mixed state $\rho_{\rm anc}=\mathbb{1}$; (ii) evolve the system and ancilla together using L CNOT gates and L SWAP gates applied as in the figure; (iii) measure the ancilla in the $\{|\pm\rangle=(|0\rangle\pm|1\rangle)/\sqrt{2}\}$ basis. The sequence (i)–(iii) defines one "time step" where time t advances by 1. We write $Q_k(t)$ for the number of measurement outcomes of type $k\in\{+,-\}$ up to time t, noting that $Q_+(t)+Q_-(t)=t$.

To postselect states conditioned on $Q_k(t)$, we employ large-deviation methods for quantum open dynamics [38,41,43,55]. Specifically, in order to postselect to change the average of $Q_+(t)-Q_-(t)$ we tilt the channel by a counting field s, such that the probabilities of measurement outcomes are reweighted by $\mathrm{e}^{s[Q_+(t)-Q_-(t)]}$. In this way, $s>0$ favors $Q_+(t)-Q_-(t)$ larger than typical, while $s<0$ disfavors it. In the notation of Fig. 1(b), this corresponds to replacing the Hadamard rotated gray bullet in the figure by a measurement (or tilting) matrix

$$= H d_s H =: m_s, \tag{1}$$

where $d_s=\mathrm{diag}(e^s,e^{-s})$. The resulting tilted channel is then

$\mathcal{M}_s =$. (2)

Dominant eigenmatrices of $\mathcal{M}_s$. For large t, the behavior of postselected trajectories is controlled by the leading eigenmatrices of the tilted channel and of its adjoint, $\mathcal{M}_s^\dagger$. Using the properties of CNOT gates, we show [56] that these leading eigenmatrices are

$$\mathcal{M}_s[\mathbb{1}]=e^{\theta(s)}\mathbb{1},\quad \mathcal{M}_s^\dagger[\rho_s^\triangleleft]=e^{\theta(s)}\rho_s^\triangleleft, \tag{3}$$

with

$$\theta(s)=\ln(2\cosh s)=\ln \mathrm{Tr}[m_s], \tag{4}$$

and where

$$\rho_s^\triangleleft := \mathcal{U}^\triangleleft\big(m_s^{\otimes L}\big)e^{-L\theta(s)} \tag{5}$$

is defined from the action of the superoperator

$\mathcal{U}^\triangleleft =$. (6)

From Eqs. (3)–(5) we deduce that $\theta(s)$ is the scaled cumulant generating function for the difference in $+$ and $-$ measurements at long times t. Its simple form arises because these measurements are independent Bernoulli random variables in the steady state of the original channel $\mathcal{M}$. Despite this simplicity, we now show that the states conditioned on these measurements are rich and complex.

Quantum Doob transform. The tilted channel is not trace preserving, $\mathcal{M}_{s\neq0}^\dagger[\mathbb{1}]\neq\mathbb{1}$. We therefore apply the quantum Doob transformation [38,41] to obtain a physical (trace-preserving) channel $\mathcal{M}_s^{\rm D}$ that reproduces the tilted ensemble

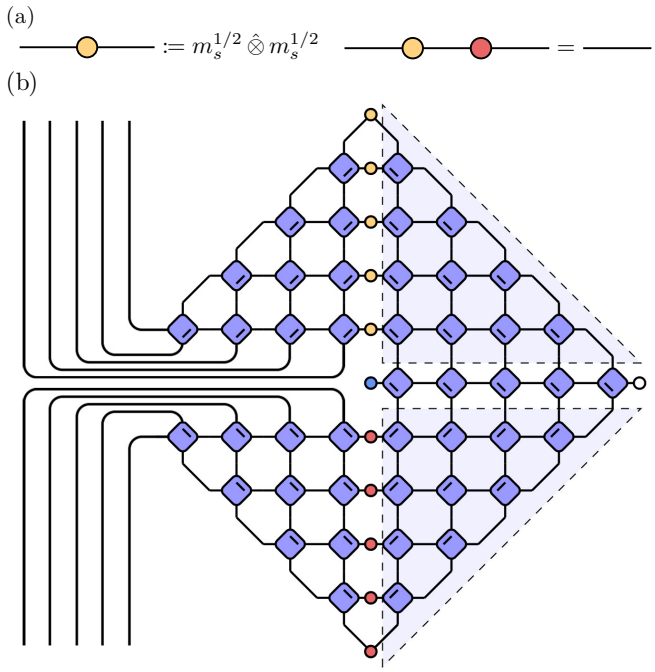


FIG. 2. Doob channel. (a) Measurement superoperators Eq. (9) and their inverses. (b) Tensor network representation of the Doob channel $\mathcal{M}_s^{\mathrm{D}}$.

of trajectories. The standard procedure leads to [56]

$$\mathcal{M}_s^{\mathrm{D}} := e^{-\theta(s)}\, \mathcal{V}_s \circ \mathcal{M}_s \circ \mathcal{V}_s^{-1}, \tag{7}$$

where $\circ$ denotes composition of superoperators, and

$$\begin{aligned} \mathcal{V}_s(\cdot) &= (\rho_s^{\triangleleft})^{1/2}(\cdot)(\rho_s^{\triangleleft})^{1/2} \\ &= e^{-L\theta(s)} \mathcal{U}^{\triangleleft} \circ \left(m_s^{1/2} \hat{\otimes} m_s^{1/2}\right)^{\otimes L} \circ \mathcal{U}^{\triangleleft}(\cdot). \end{aligned} \tag{8}$$

Note that $m_s^{1/2}$ is well defined (m_s is positive definite), and $\hat{\otimes}$ denotes the "fold" tensor product, meaning that action of the single-qubit superoperator is

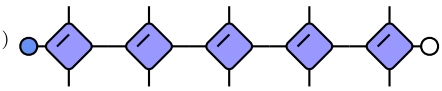
$$\left(m_s^{1/2} \hat{\otimes} m_s^{1/2}\right)[\cdot] = m_s^{1/2}(\cdot)\, m_s^{1/2}. \tag{9}$$

Figure 2 shows Eq. (7) in tensor network form, with $\mathcal{V}_s(\cdot)$ given by Eq. (8). The diagram involves four triangles, each representing $\mathcal{U}^{\triangleleft}$ [cf. Eq. (6)], and $2L$ two-legged circles, each representing $m_s^{1/2} \hat{\otimes} m_s^{1/2}$, since each $\mathcal{V}_s$ in Eq. (7) involves two of the former and L of the latter.

The Doob channel is trace preserving: its right fixed point (steady state) is $\rho_s^{\triangleleft}$ and that of its adjoint is the identity. Equations (5) and (6) express the steady state $\rho_s^{\triangleleft}$ as a linear-depth circuit which encodes long-ranged system correlations, despite the fact that the original (untilted) channel was unital and the measurement outcomes have simple statistics.

Note that, although the quantum Doob transformation is a general procedure, its implementation is generally difficult as it requires knowledge of the spectrum of the tilted generator. Eq. (7) provides an exact enactment of the quantum Doob transformation in the many-body setting. In the following we will use this explicit result to exactly characterize the correlations of $\rho_s^{\triangleleft}$, but we first make a useful connection to a form of time reversal.

Doob transform as time reversal. Consider an alternative dynamics given by the linear sequential circuit shown in Fig. 1(c). In this circuit the ancilla is prepared in a mixed state $\rho_{\mathrm{anc}} = \mathrm{e}^{-\theta(s)} m_s$ [cf. the identity for the original circuit of Fig. 1(b)], and the sequence of CNOT gates runs from top to bottom. The circuit corresponds to iterated application of the new channel

$\widetilde{\mathcal{M}}_s = e^{-\theta(s)}$  .

(10)

This channel is parametrized by the field s but, contrary to $\mathcal{M}_s$, it is completely positive and trace preserving. This is seen by comparing Eq. (10) with Eq. (2), which shows that

$$\widetilde{\mathcal{M}}_s = e^{-\theta(s)} \mathcal{M}_s^{\dagger}, \tag{11}$$

so that

$$\widetilde{\mathcal{M}}_s[\rho_s^{\triangleleft}] = \rho_s^{\triangleleft}, \quad \widetilde{\mathcal{M}}_s^{\dagger}[\mathbb{1}] = \mathbb{1}. \tag{12}$$

The nontrivial mixed state of the ancilla enables these nontrivial correlations in the typical dynamics of $\widetilde{\mathcal{M}}_s$.

Comparing Eqs. (11) and (3) suggests that the typical dynamics of the new channel and the rare events of the original channel are related by time reversal. This is proved as follows. For a generic channel $\mathcal{G}$ with unique fixed point ρ_∞, the associated time-reversed (stationary) dynamics is given by the Petz recovery map [57–59]

$$\mathcal{G}^{\mathrm{P}}[\cdot] := \rho_\infty^{1/2}\, \mathcal{G}^{\dagger}[\rho_\infty^{-1/2}(\cdot)\rho_\infty^{-1/2}]\rho_\infty^{1/2}. \tag{13}$$

For $\mathcal{G} = \widetilde{\mathcal{M}}_s$ and using Eqs. (7), (11), and (12) we get

$$\mathcal{M}_s^{\mathrm{D}} = \widetilde{\mathcal{M}}_s^{\mathrm{P}}. \tag{14}$$

Note that this correspondence between the Doob transform of the map in Eq. (2) and the Petz map of the (different) channel in Eq. (10) is nontrivial and depends on the specific form of the channels. Physically, it means that quantum trajectories of the conditional state under the Doob channel $\mathcal{M}_s^{\mathrm{D}}$ are those of $\widetilde{\mathcal{M}}_s$ but time reversed, and their stationary states coincide.

More generally, the connection to the Petz map highlights the complexity of the postselection problem for $\mathcal{M}_s$: it can be solved by the Doob channel of Fig. 2 (where the difficulty is finding the leading left eigenmatrix of $\mathcal{M}_s$), or by building the simpler channel $\widetilde{\mathcal{M}}_s$ and then time reversing its dynamics (where the difficulty is computing the Petz map). Either procedure leads to the same $\rho_s^{\triangleleft}$ and the same tilted ensemble of conditional state trajectories.

Time-inhomogeneous tilting. We can show [56] that the steady state in Eq. (12) is reached in a finite number of applications of $\widetilde{\mathcal{M}}_s$ (or alternatively $\mathcal{M}_s^{\mathrm{D}}$), specifically in $t = L$ time steps. This implies that, when thought of as a matrix, $\widetilde{\mathcal{M}}_s$ has a special structure: its spectrum is $\{0, 1\}$, the eigenvalue 1 is nondegenerate, and the largest Jordan block corresponding to the eigenvalue 0 has size L. In fact, an even stronger fact holds [56]: as long as we use tilting matrices of the form Eq. (1) the same structure is found for all s. This means that even when considering different tilt parameters $(s_1 \cdots s_t)$ at each time step t, the state at time $t \geqslant L$ is given by a form

similar to that of Eq. (5),

$$\rho_{t\geqslant L} = \widetilde{\mathcal{M}}_{s_t}\big[\cdots\widetilde{\mathcal{M}}_{s_1}[\rho_0]\big] = \mathcal{U}^{\triangleleft}\big(m_{s_t}\otimes\cdots\otimes m_{s_{t-L+1}}\big)e^{-\sum_{t'=t-L+1}^{t}\theta(s_{t'})}, \tag{15}$$

which is independent of the initial condition ρ_0. This means that after L steps this process loses all memory of the initial condition and only retains information of the last L tilting matrices.

Long-ranged correlations in the conditioned state. We now show that in contrast to the trivial stationary state of $\mathcal{M}$, when conditioning on measurements, the state develops long-range correlations. Consider a system operator O. Its expectation value at some intermediate time t over postselected trajectories that run between times 0 and T can be obtained from the tilted channel as [38,41]

$$\langle O(t)\rangle_s := \frac{\mathrm{Tr}\big(\mathcal{M}_s^{T-t}\big[O\mathcal{M}_s^t[\rho_0]\big]\big)}{\mathrm{Tr}\big(\mathcal{M}_s^T[\rho_0]\big)}. \tag{16}$$

In the limit of long times ($t, T\to\infty$ at fixed ratio $t/T<1$) we can use the fixed point structure [Eqs. (3)–(5)] to obtain at stationarity

$$\langle O\rangle_s = \mathrm{Tr}\big[\mathcal{U}^{\triangleleft}(O)m_s^{\otimes L}\big]\mathrm{e}^{-L\theta(s)}. \tag{17}$$

Given the finite convergence time of the circuit [cf. Eq. (15)], the above expression actually holds for any $L\leqslant t\leqslant T-L$. Moreover, due to Eq. (14), these are also the steady state correlations of the circuit $\widetilde{\mathcal{M}}_s$.

Consider the operator X_i that acts as Pauli σ^x on site i and trivially on all other sites. One can show [56] (where we label sites $i=0,\ldots,L-1$) that

$$\tilde{X}_i := \mathcal{U}^{\triangleleft}(X_i) = \prod_{k=0}^{i} X_k^{\beta_{i,k}}, \tag{18}$$

where $\beta_{i,k}=\binom{i}{k} \bmod 2$ is the Sierpiński triangle. With Eq. (18), using Eq. (17) we can calculate the one- and two-point correlations of X_i,

$$\langle X_i\rangle_s = \exp\left[q(s)\sum_{k=0}^{i}\beta_{i,k}\right], \tag{19}$$

$$\langle X_iX_j\rangle_s = \exp\left\{q(s)\left[\sum_{k=0}^{i}(\beta_{i,k}\oplus\beta_{j,k})+\sum_{k=i+1}^{j}\beta_{j,k}\right]\right\}, \tag{20}$$

where we consider $i<j$ and $s>0$, we have introduced $\beta\oplus\beta' = (\beta+\beta') \bmod 2$, and $q(s)=\ln\tanh(s)$. For $s<0$ the same formulas hold but q is complex [$\mathrm{Im}(q)=\pi$]. Therefore, while the expectation values are still real they can be negative. For $s\to 0$, $\mathrm{Re}(q)\to-\infty$ and the expectation values above vanish (except for $i=j$), reflecting that $\rho_s^{\triangleleft}\to\mathbb{1}$ in this limit. In the limit $s\to\infty$ we have $q(s)\to 0$ and both expectation values approach unity, reflecting that $\rho_s^{\triangleleft}\to|+\rangle\langle+|^{\otimes L}$.

The result for $\langle X_i\rangle_s$ means that the system has no "bulk," i.e., far from the origin, this one-point function is close to zero at most sites, but there are some special sites where it stays of order unity: for example, $\langle X_i\rangle_s=\mathrm{e}^{2q(s)}$ for $i=2^m$.

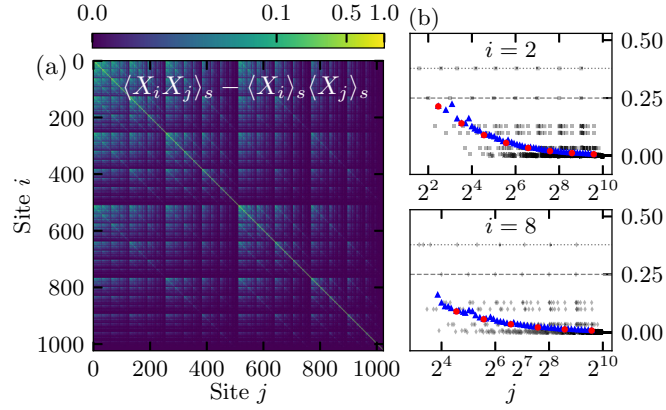


FIG. 3. (a) Correlation function $C_s(i,j)$ for $s=0.9$ and $L=1024$. (b) $C_s(i,j)$ as a function of $j>i$ for fixed $i=2$ (top) and $i=8$ (bottom). The gray dashed and dotted horizontal lines indicate the values of $C_s(2^m,2^n)$ and $C_s(2^m,2^n+2^m)$. The red circles are the averages $[C_s(i,\cdot)]_{2^n}^{2^{n+1}}$. The blue triangles are $[C_s(i,\cdot)]_{2^{(n/8)}}^{2^{(n/8)+1}}$.

To understand the "typical" behavior of the correlators, we average them over spatial windows, as follows. Recalling Eq. (19) we consider $V_j=\sum_{k=0}^{j}\beta_{j,k}$ which is the number of 1's in the jth row of the Sierpiński's triangle. We take $L=2^m$ and average the kth power of V_j over rows j between 0 and $L-1$ to obtain [56]

$$[V^k]_0^L = \left(\frac{1+2^k}{2}\right)^m = L^{d_{\mathfrak{f}}(k)-1}, \tag{21}$$

where $[(\cdot)]_a^b := (b-a)^{-1}\sum_{j=a}^{b-1}(\cdot)_j$ is the windowed average, and $d_{\mathfrak{f}}(k) := \ln(1+2^k)/\ln 2$ [so $d_{\mathfrak{f}}(1)\approx 1.584$ is the fractal dimension of the Sierpiński triangle]. This gives the following averaged one-point function,

$$[\langle X\rangle_s]_0^L = \frac{1}{2^m}\sum_{j=0}^{m}\binom{m}{j}e^{2^jq(s)} \geqslant \frac{e^{q(s)}}{L}. \tag{22}$$

A similar fractal structure is also observed in the connected two-point function,

$$C_s(i,j) = \langle X_iX_j\rangle_s - \langle X_i\rangle_s\langle X_j\rangle_s. \tag{23}$$

For instance, Fig. 3 shows that there exist pairs of sites with arbitrarily large separation and C_s of order unity, indicating infinite-ranged correlations. From Eq. (20) we have that for positive integers $m\neq n$,

$$C_s(2^m,2^n) = e^{2q(s)}-e^{4q(s)}, \tag{24}$$

$$C_s(2^m,2^n+2^m) = e^{2q(s)}-e^{6q(s)}, \tag{25}$$

which do not decay as m,n increase (see Fig. 3).

On the other hand, taking $i=2^m$ and averaging j in the window $[2^n,2^{n+1}-1]$ with $n>m$, we find [56]

$$[C_s(2^m,\cdot)]_{2^n}^{2^{n+1}} = \frac{1}{2^n}\sum_{j=0}^{n-1}\binom{n-1}{j}\big(e^{2^{j+2}q(s)} - 2\sinh[2q(s)]e^{2^{j+1}q(s)}\big) + \frac{e^{2(2^n+1)q(s)}}{2^n}. \tag{26}$$

This average provides an estimate of the typical correlations in the conditioned state of Eq. (5) (see Fig. 3). These spatially averaged correlations decay algebraically with the window size (which is 2^n); they are independent of m so this two-body correlation is primarily determined by the absolute distance from the origin and not the distance between the qubits. We note that while $\rho_s^{\triangleleft}$ has long-ranged correlations, these are classical in nature as the state is separable (it is diagonal in the X basis).

Discussion. Here, we have calculated exactly the dynamical large deviations of measurements at the boundary of a sequential quantum East circuit. Despite the fact that the stationary state is trivial and the measurements a Bernoulli process, we have shown that when the final state is conditioned (specifically, exponentially tilted) on the measurement outcomes it contains long-range correlations. This is a form of boundary-bulk correspondence, where acting on the system's boundary one can control its bulk properties. Our result here is one of the very few examples of an exact characterization of dynamical large deviations in a genuine many-body system.

We have also found an interesting connection to time reversal, where the "Doob dynamics" that optimally samples the rare events of the circuit corresponds to the Petz recovery map that time reverses the dynamics of a different circuit whose environment is structured. As for the large deviations, this result is a rare example of the exact solution of a Petz map in a many-body problem.

The circuit we study can be realized in current quantum devices as it requires only CNOT and SWAP gates together with midcircuit measurements [60]. Our results provide a way to create long-range correlated states simply by controlling a boundary ancilla. Being exact, our results can also serve as a benchmark for experimental devices. While the correlations we have shown here are only classical, a similar setting could be used to generate genuine entanglement by simply introducing measurements at the opposite end [56]. We hope to report a systematic study on this and other extensions in future work [61–69].

Acknowledgments. J.L. acknowledges support by the UKRI Grant No. EP/Z003342/1. B.B. acknowledges financial support from the Royal Society through the University Research Fellowship No. 201101. J.P.G. acknowledges financial support from EPSRC Grant No. EP/V031201/1 and Leverhulme Trust Grant No. RPG-2024-112.

Data availability. The data that support the findings in this Letter are available from the authors upon reasonable request.

[1] A. C. Potter and R. Vasseur, Entanglement dynamics in hybrid quantum circuits, in *Entanglement in Spin Chains: From Theory to Quantum Technology Applications*, edited by A. Bayat, S. Bose, and H. Johannesson (Springer, Cham, 2022), pp. 211–249.

[2] M. P. Fisher, V. Khemani, A. Nahum, and S. Vijay, Random quantum circuits, Annu. Rev. Condens. Matter Phys. **14**, 335 (2023).

[3] B. Bertini, P. W. Claeys, and T. Prosen, Exactly solvable many-body dynamics from space-time duality, arXiv:2505.11489.

[4] H.-R. Wang, X.-Y. Yang, and Z. Wang, Exact hidden Markovian dynamics in quantum circuits, Phys. Rev. Lett. **133**, 170402 (2024).

[5] Z. Wang, Hopf algebras and solvable unitary circuits, Phys. Rev. B **111**, 104315 (2025).

[6] X.-H. Yu, Z. Wang, and P. Kos, Hierarchical generalization of dual unitarity, Quantum **8**, 1260 (2024).

[7] S. J. Evered, D. Bluvstein, M. Kalinowski, S. Ebadi, T. Manovitz, H. Zhou, S. H. Li, A. A. Geim, T. T. Wang, N. Maskara, *et al.*, High-fidelity parallel entangling gates on a neutral-atom quantum computer, Nature (London) **622**, 268 (2023).

[8] J.-S. Chen, E. Nielsen, M. Ebert, V. Inlek, K. Wright, V. Chaplin, A. Maksymov, E. Páez, A. Poudel, P. Maunz, and J. Gamble, Benchmarking a trapped-ion quantum computer with 30 qubits, Quantum **8**, 1516 (2024).

[9] C. M. Löschnauer, J. M. Toba, A. C. Hughes, S. A. King, M. A. Weber, R. Srinivas, R. Matt, R. Nourshargh, D. T. C. Allcock, C. J. Ballance, C. Matthiesen, M. Malinowski, and T. P. Harty, Scalable, high-fidelity all-electronic control of trapped-ion qubits, PRX Quantum **6**, 040313 (2025).

[10] L. E. Fischer, M. Leahy, A. Eddins, N. Keenan, D. Ferracin, M. A. C. Rossi, Y. Kim, A. He, F. Pietracaprina, B. Sokolov, S. Dooley, Z. Zimborás, F. Tacchino, S. Maniscalco, J. Goold, G. García-Pérez, I. Tavernelli, A. Kandala, and S. N. Filippov, Dynamical simulations of many-body quantum chaos on a quantum computer, Nat. Phys. **22**, 302 (2026).

[11] R. Acharya, D. A. Abanin, L. Aghababaie-Beni, I. Aleiner, T. I. Andersen, *et al.*, Quantum error correction below the surface code threshold, Nature (London) **638**, 920 (2025).

[12] F. Baccari, P. Kos, and G. Styliaris, Average-computation benchmarking for local expectation values in digital quantum devices, arXiv:2507.18708.

[13] B. Skinner, J. Ruhman, and A. Nahum, Measurement-induced phase transitions in the dynamics of entanglement, Phys. Rev. X **9**, 031009 (2019).

[14] Y. Li, X. Chen, and M. P. A. Fisher, Measurement-driven entanglement transition in hybrid quantum circuits, Phys. Rev. B **100**, 134306 (2019).

[15] J. C. Hoke, M. Ippoliti, E. Rosenberg, D. Abanin, *et al.*, Measurement-induced entanglement and teleportation on a noisy quantum processor, Nature (London) **622**, 481 (2023).

[16] L. Piroli, G. Styliaris, and J. I. Cirac, Quantum circuits assisted by local operations and classical communication: Transformations and phases of matter, Phys. Rev. Lett. **127**, 220503 (2021).

[17] G.-Y. Zhu, N. Tantivasadakarn, A. Vishwanath, S. Trebst, and R. Verresen, Nishimori's cat: Stable long-range entanglement from finite-depth unitaries and weak measurements, Phys. Rev. Lett. **131**, 200201 (2023).

[18] M. Iqbal, N. Tantivasadakarn, T. M. Gatterman, J. A. Gerber, K. Gilmore, D. Gresh, A. Hankin, N. Hewitt, C. V. Horst, M. Matheny, *et al.*, Topological order from measurements and feed-forward on a trapped ion quantum computer, Commun. Phys. **7**, 205 (2024).

[19] S. Gopalakrishnan, Push-down automata as sequential generators of highly entangled states, arXiv:2305.04951.

[20] T.-C. Lu, S. Gopalakrishnan, and Y. You, Spacetime duality between sequential and measurement-feedback circuits, arXiv:2507.12523.
[21] J. Lloyd and D. A. Abanin, Quantum thermal state preparation for near-term quantum processors, arXiv:2506.21318.
[22] Z. Ding, C.-F. Chen, and L. Lin, Single-ancilla ground state preparation via Lindbladians, Phys. Rev. Res. **6**, 033147 (2024).
[23] F. Ciccarello, S. Lorenzo, V. Giovannetti, and G. M. Palma, Quantum collision models: Open system dynamics from repeated interactions, Phys. Rep. **954**, 1 (2022).
[24] D. Cilluffo, G. Buonaiuto, I. Lesanovsky, A. Carollo, S. Lorenzo, G. M. Palma, F. Ciccarello, and F. Carollo, Microscopic biasing of discrete-time quantum trajectories, Quantum Sci. Technol. **6**, 045011 (2021).
[25] M. Cech, I. Lesanovsky, and F. Carollo, Thermodynamics of quantum trajectories on a quantum computer, Phys. Rev. Lett. **131**, 120401 (2023).
[26] M. Cech, M. Cea, M. C. Bañuls, I. Lesanovsky, and F. Carollo, Space-time correlations in monitored kinetically constrained discrete-time quantum dynamics, Phys. Rev. Lett. **134**, 230403 (2025).
[27] M. Cech, C. D. Fazio, M. Cea, M. C. Bañuls, I. Lesanovsky, and F. Carollo, Revealing emergent many-body phenomena by analyzing large-scale space-time records of monitored quantum systems, arXiv:2507.00944.
[28] J. I. Cirac, D. Pérez-García, N. Schuch, and F. Verstraete, Matrix product states and projected entangled pair states: Concepts, symmetries, theorems, Rev. Mod. Phys. **93**, 045003 (2021).
[29] C. Schön, E. Solano, F. Verstraete, J. I. Cirac, and M. M. Wolf, Sequential generation of entangled multiqubit states, Phys. Rev. Lett. **95**, 110503 (2005).
[30] C. Schön, K. Hammerer, M. M. Wolf, J. I. Cirac, and E. Solano, Sequential generation of matrix-product states in cavity QED, Phys. Rev. A **75**, 032311 (2007).
[31] M. C. Bañuls, D. Pérez-García, M. M. Wolf, F. Verstraete, and J. I. Cirac, Sequentially generated states for the study of two-dimensional systems, Phys. Rev. A **77**, 052306 (2008).
[32] Z.-Y. Wei, D. Malz, and J. I. Cirac, Sequential generation of projected entangled-pair states, Phys. Rev. Lett. **128**, 010607 (2022).
[33] V. Belavkin, A stochastic posterior Schrödinger equation for counting nondemolition measurement, Lett. Math. Phys. **20**, 85 (1990).
[34] H. Carmichael, *An Open Systems Approach to Quantum Optics*, Lecture Notes in Physics Vol. 18 (Springer, Berlin, 1993).
[35] C. Gardiner and P. Zoller, *Quantum Noise* (Springer, Berlin, 2004).
[36] M. B. Plenio and P. L. Knight, The quantum-jump approach to dissipative dynamics in quantum optics, Rev. Mod. Phys. **70**, 101 (1998).
[37] H. P. Breuer and F. Petruccione, *The Theory of Open Quantum Systems* (Oxford University Press, Oxford, U.K., 2002).
[38] J. P. Garrahan and I. Lesanovsky, Thermodynamics of quantum jump trajectories, Phys. Rev. Lett. **104**, 160601 (2010).
[39] M. Esposito, U. Harbola, and S. Mukamel, Nonequilibrium fluctuations, fluctuation theorems, and counting statistics in quantum systems, Rev. Mod. Phys. **81**, 1665 (2009).
[40] J. P. Garrahan, Aspects of non-equilibrium in classical and quantum systems: Slow relaxation and glasses, dynamical large deviations, quantum non-ergodicity, and open quantum dynamics, Physica A **504**, 130 (2018).
[41] F. Carollo, J. P. Garrahan, I. Lesanovsky, and C. Pérez-Espigares, Making rare events typical in Markovian open quantum systems, Phys. Rev. A **98**, 010103(R) (2018).
[42] H. Touchette, The large deviation approach to statistical mechanics, Phys. Rep. **478**, 1 (2009).
[43] F. Carollo, R. L. Jack, and J. P. Garrahan, Unraveling the large deviation statistics of Markovian open quantum systems, Phys. Rev. Lett. **122**, 130605 (2019).
[44] D. Berenstein and J. Zhao, Exotic equilibration dynamics on a 1-D quantum CNOT gate lattice, arXiv:2102.05745.
[45] K. Klobas, C. De Fazio, and J. P. Garrahan, Exact pretransition effects in kinetically constrained circuits: Dynamical fluctuations in the Floquet-East model, Phys. Rev. E **110**, L022101 (2024).
[46] B. Bertini, P. Kos, and T. Prosen, Localized dynamics in the Floquet quantum East model, Phys. Rev. Lett. **132**, 080401 (2024).
[47] B. Bertini, C. De Fazio, J. P. Garrahan, and K. Klobas, Exact quench dynamics of the Floquet quantum East model at the deterministic point, Phys. Rev. Lett. **132**, 120402 (2024).
[48] J. Iaconis, S. Vijay, and R. Nandkishore, Anomalous subdiffusion from subsystem symmetries, Phys. Rev. B **100**, 214301 (2019).
[49] Y. Le Gal, X. Turkeshi, and M. Schirò, Entanglement dynamics in monitored systems and the role of quantum jumps, PRX Quantum **5**, 030329 (2024).
[50] Y. Han and X. Chen, Entanglement dynamics in U(1) symmetric hybrid quantum automaton circuits, Quantum **7**, 1200 (2023).
[51] X. Feng and M. Ippoliti, Dynamics of pseudoentanglement, J. High Energy Phys. 02 (2025) 128.
[52] D. Szász-Schagrin, M. Mazzoni, B. Bertini, K. Klobas, and L. Piroli, Entanglement dynamics and Page curves in random permutation circuits, Phys. Rev. Res. **8**, L012061 (2026).
[53] B. T. McDonough, C. Chamon, J. H. Wilson, and T. Iadecola, Bridging classical and quantum information scrambling with the operator entanglement spectrum, Quantum **10**, 2012 (2026).
[54] B. Bertini, K. Klobas, P. Kos, and D. Malz, Random permutation circuits are quantum chaotic, Phys. Rev. B **113**, L100302 (2026).
[55] J. Li, R. L. Jack, B. Bertini, and J. P. Garrahan, Efficient post-selection in light cone correlations of monitored quantum circuits, Phys. Rev. B **111**, 024309 (2025).
[56] See Supplemental Material at http://link.aps.org/supplemental/10.1103/72kx-56lt for more details, which includes Refs. [61–69].
[57] D. Petz, Sufficient subalgebras and the relative entropy of states of a von Neumann algebra, Commun. Math. Phys. **105**, 123 (1986).
[58] H. Kwon, R. Mukherjee, and M. S. Kim, Reversing Lindblad dynamics via continuous Petz recovery map, Phys. Rev. Lett. **128**, 020403 (2022).
[59] G. Bai, F. Buscemi, and V. Scarani, Quantum Bayes' rule and Petz transpose map from the minimum change principle, Phys. Rev. Lett. **135**, 090203 (2025).
[60] K. Rudinger, G. J. Ribeill, L. C. G. Govia, M. Ware, E. Nielsen, K. Young, T. A. Ohki, R. Blume-Kohout, and T. Proctor, Characterizing mid-circuit measurements on a superconducting qubit using gate set tomography, arXiv:2103.03008.

[61] L. Piroli and J. I. Cirac, Quantum cellular automata, tensor networks, and area laws, Phys. Rev. Lett. **125**, 190402 (2020).

[62] M. A. Nielsen and I. L. Chuang, *Quantum Computation and Quantum Information* (Cambridge University Press, Cambridge, U.K., 2010).

[63] H. Touchette, Introduction to dynamical large deviations of Markov processes, Physica A **504**, 5 (2018).

[64] R. L. Jack, Ergodicity and large deviations in physical systems with stochastic dynamics, Eur. Phys. J. B **93**, 74 (2020).

[65] S. Gopalakrishnan and A. Lamacraft, Unitary circuits of finite depth and infinite width from quantum channels, Phys. Rev. B **100**, 064309 (2019).

[66] G. Giudice, G. Giudici, M. Sonner, J. Thoenniss, A. Lerose, D. A. Abanin, and L. Piroli, Temporal entanglement, quasiparticles and the role of interactions, Phys. Rev. Lett. **128**, 220401 (2022).

[67] V. Popkov, G. M. Schütz, and D. Simon, ASEP on a ring conditioned on enhanced flux, J. Stat. Mech. (2010) P10007.

[68] R. L. Jack, I. R. Thompson, and P. Sollich, Hyperuniformity and phase separation in biased ensembles of trajectories for diffusive systems, Phys. Rev. Lett. **114**, 060601 (2015).

[69] B. Buča, J. P. Garrahan, T. Prosen, and M. Vanicat, Exact large deviation statistics and trajectory phase transition of a deterministic boundary driven cellular automaton, Phys. Rev. E **100**, 020103(R) (2019).